Manuscript submitted May 30, 1984; revised manuscript received *ca.* Dec. 5, 1984.

REFERENCES

1. M. Keddam, J. F. Lizee, C. Pallotta, and H. Takenouti, *This Journal*, **131**, 2106 (1984).
2. A. C. Makrides, *ibid.*, **111**, 392 (1964).
3. W. Schmickler, in "Passivity of Metals," R. P. Frankenthal and J. Kruger, Editors, p. 102, The Electrochemical Society Corrosion Monograph Series, Princeton, NJ (1978).
4. F. N. Delnick and N. Hackerman, in "Passivity of Metals," R. P. Frankenthal and J. Kruger, Editors, p. 116, The Electrochemical Society Corrosion Monograph Series, Princeton, NJ (1978).
5. V. Stimming and J. W. Schultze, *Electrochim. Acta*, **24**, 859 (1979).
6. W. Schmickler, in "Fifth International Symposium on Passivity," p. 23, Société de Chimie Physique, Bombannes, France (1983).
7. C. Deslouis, C. Gabrielli, Ph. Sainte-Rose Franchine, and B. Tribollet, *This Journal*, **129**, 107 (1982).
8. C. Deslouis, C. Gabrielli, and B. Tribollet, *ibid.*, **130**, 2044 (1983).
9. B. Tribollet and J. Newman, *ibid.*, **130**, 2016 (1983).
10. C. Deslouis, M. Duprat, M. Keddam, F. Moran, and B. Tribollet, Abstract 198, p. 306, The Electrochemical Society Extended Abstracts, Vol. 83-2, Washington, DC, Oct. 9-14, 1983.
11. R. C. Alkire and S. Perusich, *Corros. Sci.*, **23**, 1121 (1983).
12. M. Nagayama and M. Cohen, *This Journal*, **110**, 670 (1963).
13. M. Nagayama and S. Kawamura, *Electrochim. Acta.*, **12**, 1109 (1967).
14. M. Keddam, J. F. Lizée, C. D. Pallotta, and H. Takenouti, in "Fifth International Symposium on Passivity," p. 51, Société de Chimie Physique, Bombannes, France (1983).
15. P. Pascal "Nouveau Traité de Chimie Minérale," Tome XVII, pp. 615-687, M. Masson, Editor, Paris (1967).
16. R. Dupeyrat, M. Froelicher, A. Hugot-Le Goff, M. Masson, and C. Pallotta, in "Fifth International Symposium on Passivity," p. 101, Société de Chimie Physique, Bombannes, France (1983)
17. J. W. Essam, *Rep. Prog. Phys.*, **43**, 834 (1980).
18. A. Breewsma and J. Lyklema, *Discuss. Faraday Soc.*, **52**, 324 (1971).
19. A. Breewsma and J. Lyklema, *J. Colloid Interface Sci.*, **43**, 437 (1973).
20. L. Bolistrien and J. Murray, in "Chemical Modeling in Aqueous Systems," E. A. Jenne, Editor, Chap. 14, ACS Symposium Series 93, American Chemical Society, Washington, DC (1979).
21. A. Davis and J. O. Leckie, *J. Colloid Interface Sci.*, **74**, 32 (1980).
22. S. Kittaka and T. Morimoto, *ibid.*, **75**, 398 (1980).
23. F. Y. Onoda and P. L. De Bruyn, *Surf. Sci.*, **4**, 48 (1966).
24. G. A. Parks and P. L. De Bruyn, *J. Phys. Chem.*, **66**, 967 (1962).
25. T. Sugimoto and E. Matijevic, *J. Colloid Interface Sci.*, **74**, 227 (1980).
26. M. Kiyama and T. Takada, *Bull. Chem. Soc. Jpn.*, **45**, 1923 (1972); T. Ishikawa and K. Inouye, *ibid.*, **45**, 2350 (1972); S. Music, A. Vertes, G. Simmons, I. Czakó-Nagy, and A. Leidheiser, *J. Colloid Interface Sci.*, **85**, 256 (1982).
27. E. Matijevic, *Corrosion*, **35**, 264 (1979).
28. F. Dumont and A. Watillon, *Discuss. Faraday Soc.*, **52**, 352 (1971).
29. F. J. Hingston, A. M. Posner, and J. P. Quirk, *ibid.*, **52**, 334 (1971).
30. A. Hugot-LeGoff and C. Pallotta, Submitted to *This Journal*.
31. W. Revie, B. G. Baker, and J. O'M. Bockris, *This Journal*, **122**, 1460 (1975).
32. W. E. O'Grady, *ibid.*, **127**, 555 (1980).
33. R. W. Hoffman, in "Fifth International Symposium on Passivity," p. 147, Société de Chimie Physique, Bombannes, France (1983).
34. R. Berneron, J. C. Charbonnier, R. Namdai-Irani, and J. Manenc, *Corros. Sci.*, **20**, 899 (1980).

Ellipsometric Study of Anodic Oxide Films on Titanium in Hydrochloric Acid, Sulfuric Acid, and Phosphate Solution

Toshiaki Ohtsuka, Minoru Masuda, and Norio Sato*

Electrochemistry Laboratory, Faculty of Engineering, Hokkaido University, Sapporo 060, Japan

ABSTRACT

The anodic oxide film on titanium has been studied by ellipsometry and SEM observation. *Ex situ* multiple-angle-of-incidence and *in situ* ellipsometric measurements allow the complex refractive index to be estimated at $\bar{n} = 2.3\text{-}2.9i$ for the titanium substrate and at $\bar{n} = 2.1\text{-}0.03i$ for the anodic oxide film at wavelength 546.1 nm. The anodic oxide film thickness increases linearly with potential in a range from −0.55 to 7.5V (RHE) at the rate of 2.8 nm V^{-1} in phosphate solutions of *p*H 1.6-12.1, 2.5 nm V^{-1} in 0.1*M* HCl solution, and 2.4 nm V^{-1} in 0.1*M* H_2SO_4 solution. At potentials more positive than 7.5V, the film breaks down, leading to the formation of a thick oxide film probably due to an increased ionic current through the breakdown sites. The film composition is estimated to be $TiO_2(H_2O)_{1.4}$ or $TiO_{0.6}(OH)_{2.8}$, which suggests the presence of hydroxyl bridge in its bonding structure.

The physicochemical properties of anodic oxide films formed on titanium are of importance in understanding the corrosion stability and photoelectrochemical activity of titanium oxide and oxide-covered titanium, which have attracted interest in recent years in the field of photoelectrode materials.

There has been a number of studies on the passivation of titanium dealing with the mechanism of active dissolution and active-passive transition in acidic aqueous media from electrochemical and impedance measurements (1-6). Armstrong *et al.* (1) and Harrison *et al.* (7) found that titanium dissolves producing Ti (III) ion in the active potential region and Ti (IV) ion in the passive potential region. Impedance measurements have shown that the electrode capacitance of titanium decreases when the passivation manifests itself on the polarization curve (1, 7). The film formation accompanying passivation was investigated in aqueous and anhydrous solutions by Laser *et al.* (8) and Smith *et al.* (9) using ellipsometry.

Many attempts have also been made to produce thick oxide films by anodization at high current efficiency. In some respects, titanium behaves as a typical valve metal, but the anodic oxide film is electrochemically less stable than the barrier films formed on Al, Ta, and Nb (10). McAleer *et al.* (10) investigated by optical interferometry the breakdown phenomenon during potentiostatic anodization of titanium at high scan rate and found that both oxygen evolution and rapid film thickening take place when the film breaks down. Yahalom *et al.* (11) investigated by use of TEM the anodic oxide film of titanium stripped from the metal substrate and detected the anatase type of diffraction pattern for the anodized oxide

*Electrochemical Society Active Member.

film subjected to breakdown and crystallization. Dyer *et al.* (12) employed ellipsometry to study the film growth on titanium during galvanostatic oxidation and obtained the relationship between film thickness, cell voltage, weight gain, and anodic charge passed.

In this work, the relation between potential and film thickness is examined for the anodic oxide films formed on titanium in aqueous solution of various *p*H values in a wide range of potential from 0 to 15V, including the passivation and anodization regions. Furthermore, the film breakdown is discussed on the basis of the thickness measurements and electron microscopic observation of the film.

Experimental

A titanium sheet of 99.85 weight percent (w/o) purity (impurity: C = 0.009, N = 0.004, O = 0.101, H = 0.0013, and Fe = 0.036%) was cut to specimens 10 × 15 mm with a small handle. The specimens were mechanically polished through to 2000 grid emery paper, degreased with acetone in an ultrasonic cleaner, and annealed in vacuum at 1030 K for 3h. They were further polished by alumina abrasives through to 0.5 μm and finally etched in an aqueous mixture of HF (2 volume percent [v/o]) and HNO_3 (4 v/o) for 2s at room temperature. After polishing, the small handle of the specimen connected with a lead wire was covered with silicon rubber sealant.

Electrolytes used are aqueous solutions of 0.1*M* (mol dm^{-3}) H_2SO_4 (*p*H 0.9), 0.1*M* HCl (*p*H 1.1), and four mixtures of 0.1*M* H_3PO_4 and 0.1*M* Na_3PO_4 (*p*H 1.6, 4.6, 6.9, and 12.1). The solutions were prepared from doubly distilled water and analytical-grade reagents. Before transfer into the cell, the solutions were deoxygenated by injecting purified nitrogen gas for more than 24h in solution reservoirs, each of which is connected with the cell through a stopcock.

The electrolytic cell was a Pyrex vessel 100 cm^3 in capacity with two optical quartz windows fixed at an angle of 140.64°.

Titanium ion dissolved into the solution during anodic oxidation was analyzed by a colorimetric method using hydrogen peroxide. All measurements were carried out at 298.3±0.5 K. The electrode potential of titanium was measured in reference to a Ag/AgCl electrode and converted into the reversible hydrogen electrode potential scale in the same solution at P_{H_2} = 1 atm (RHE).

Two types of manual ellipsometers were used, one of which was a vertical type of ellipsometer (Rudolf Company Type 43702-200E) for *ex situ* measurements in air by the multiple-angle-of-incidence (MAI) method (13) and the other a horizontal type of ellipsometer (Mizojiri Company Type DV 36) for *in situ* measurements in the electrolytic cell. For these ellipsometers, filters were used to isolate a 546.1 nm light beam for mercury lamps. The polarizer and compensator were placed in the incidence light path, and the analyzer and detector in the reflected light path. The *ex situ* MAI method was adopted to determine the optical unknown parameters of the oxide-covered titanium; *i.e.*, the complex refractive index of titanium substrate $\bar{n}_3 = n_3 - ik_3$, complex refractive index of oxide film $\bar{n}_2 = n_2 - ik_2$, and film thickness d. The MAI measurement was carried out at four different angles of incidence, ϕ_1 = 45.0°, 55.0°, 65.0°, and 75.0°, for the electrode which had been anodically oxidized, rinsed with doubly distilled water, and then stored in a desiccator at room temperature. Calculation of five unknown parameters (n_3, k_3, n_2, k_2, and d) or three unknown parameters (n_2, k_2, and d) was made to minimize the standard deviation

$$\text{std dev} = \left[\frac{\sum_{i}^{N} (2\Psi_i{}^{M} - 2\Psi_i{}^{T})^2 + (\Delta_i{}^{M} - \Delta_i{}^{T})^2}{2N-1} \right]^{1/2} \quad [1]$$

where $\Psi_i{}^{M}$ and $\Delta_i{}^{M}$ are, respectively, experimental values of the relative amplitude ratio and the relative phase difference at an angle of incidence $\phi_{1,i}$, and $\Psi_i{}^{T}$ and $\Delta_i{}^{T}$ are the theoretical values. The reason for the use of a factor of two for Ψ in Eq. [1] is that Ψ must have an error limit one-half as large as that of Δ, because the Ψ and Δ have been obtained from the azimuths of polarizer, P, and analyzer, A, under the extinction condition in what is known as the first zone: $\Psi = A$ and $\Delta = 2P + 90°$, where A and P have been measured at a similar degree of error limit. The *in situ* measurement was conducted at an angle of incidence ϕ_1 = 70.32°, and analysis was made by making experimental loci of Ψ and Δ fit theoretical curves computed using the optical parameters estimated by the MAI method. All the ellipsometric analysis calculations were carried out at Hokkaido University Computing Center (14).

Results

Polarization curve.—Figure 1 shows the anodic current density (c.d.) measured after 1h polarization of the original specimen at every designated potential in 0.1*M* HCl solution and in 0.1*M* H_2SO_4 solution. The average dissolution c.d., i_{diss}, is also plotted, which was determined from the amount of Ti(IV) ion dissolved into solution during 1h polarization in 0.1*M* H_2SO_4 solution. In 0.1*M* H_2SO_4 solution, the active-passive transition is observed to occur at −0.2V. In 0.1*M* HCl solution, however, no active dissolution is observed. The passivation manifests itself in a potential range from −0.2 to 3.0V, beyond which oxygen evolution takes place. In the oxygen evolution potential region the polarization curve exhibits the Tafel slope as large as 2.3 V decade^{-1}, which is much greater than that of other transition metals, such as iron, nickel, and cobalt. Such a large Tafel slope is probably due to the large bandgap energy of semiconductive oxide films formed on titanium. In 0.1*M* HCl solution, pitting corrosion was observed at potentials more positive than 11V, and the anodic current greater than 1×10^{-3} A cm^{-2} produced white corrosion precipitates speckling the specimen surface slightly colored dark blue due to interference of light. The average dissolution c.d. measured for 1h polarization in 0.1*M* H_2SO_4 solution increases slightly with potential, reaching 1×10^{-6} A cm^{-2} at 12V. In 0.1*M* H_2SO_4 solution, the amount of Ti dissolved in the active potential region was found to be equivalent to Ti(III) dissolution. The polarization curve was also measured in phosphate solutions, which was similar to that obtained in 0.1*M* HCl solution (see Fig. 6).

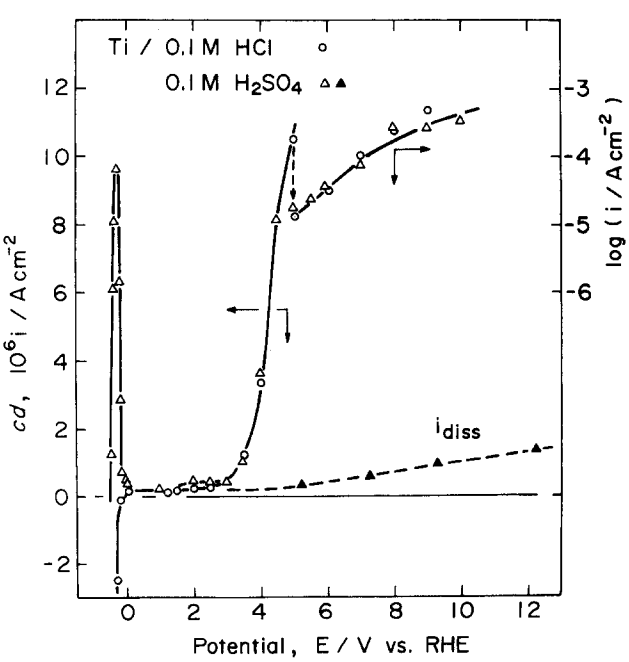

Fig. 1. Anodic current and average dissolution current as functions of potential for titanium electrode in 0.1M hydrochloric and 0.1M sulfuric acid solutions. The anodic current was measured at the end of 1h potentiostatic oxidation of the original specimen, and the average dissolution current was estimated from the amount of Ti(IV) ion dissolved into solution during 1h oxidation.

Ellipsometry.—To analyze the surface oxide film by ellipsometry, the complex refractive index, $\bar{n}_3 = n_3 - ik_3$, of the substrate metal must be known. In this work, the *ex situ* MAI method was applied to estimate the optical parameters of titanium metal and a thin air-formed oxide layer on the polished specimen surface. The result is shown in Fig. 2, where comparison is made between the measured values and the theoretical curves estimated by the least squares method. The optical parameters thus estimated with a mirror-like titanium surface provide the complex refractive index $\bar{n}_3 = 2.3\ (\pm 0.1) - 2.9(\pm 0.1)i$ for titanium metal, $\bar{n}_2 = 2.0(\pm 0.1) - 0.03\ (\pm 0.015)i$ for an air-formed oxide layer, and the film thickness $d = 2.9(\pm 0.5)$ nm. Figure 2 also shows the result obtained with a titanium electrode anodically oxidized at 7.35V in pH 6.9 phosphate solution, from which the values of $\bar{n} = 2.13\text{-}0.03i$ and $d = 25.3$ nm are determined with the above complex refractive index of titanium metal. Similar *ex situ* measurements by the MAI method were performed for a number of titanium electrodes anodically oxidized at various potentials in pH 6.9 phosphate solution and in sulfuric acid solution, and the average value of the complex refractive index of the anodic oxide film is found from the measurements to be $\bar{n}_2 = 2.2(\pm 0.1) - 0.03(\pm 0.005)i$.

Figure 3 shows the experimental loci of Ψ *vs.* Δ obtained from *in situ* ellipsometric measurements for a number of anodically oxidized titanium electrodes in a potential region from 1 to 10V in 0.1*M* HCl and 0.1*M* H_2SO_4 solutions. The solid line in Fig. 3 indicates a theoretical line along which a film with $\bar{n}_2 = 2.10\text{-}0.030i$ grows on the substrate with $\bar{n}_3 = 2.3\text{-}2.9i$. Similar loci of Ψ *vs.* Δ were obtained also in phosphate solutions at various pH values. The results are given in Fig. 4 along a theoretical line corresponding to the complex refractive index of the film formed in 0.1*M* H_2SO_4 and 0.1*M* HCl solution. As shown in Fig. 3 and 4, there is a fairly good agreement between the experimental loci and the theoretical line for the range of film thickness thinner than 30 nm. A slight deviation of the experimental loci from the theoretical line is observed for the film thicker than 30 nm, which may be attributed to the surface roughening described later. This deviation, however, appears to exert only a slight influence on the thickness estimation so that the same complex refractive index is used to evaluate the film thicker than 30 nm. The optical parameters estimated under this *in situ* condition is in agreement with the optical parameters obtained from the *ex situ* MAI measurement, except for a small difference in the refractive index of the oxide film, n_2. The change of the oxide film that might occur during storage was checked by MAI ellipsometry after removal of the specimen from the electrochemical cell and found to be inappreciable after 5 days of storage in desiccator.

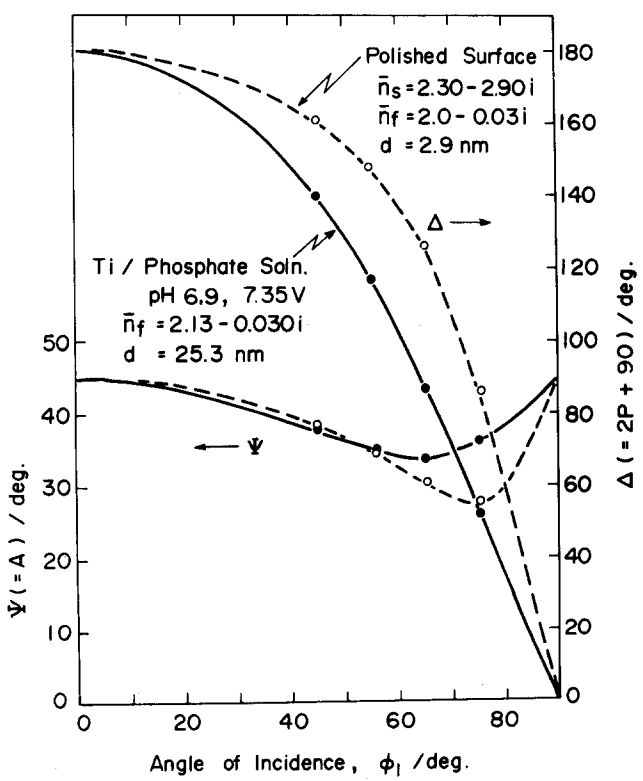

Fig. 2. Comparison between experimental Ψ and Δ at multiple angles of incidence and theoretical curves calculated from the optimum values of thickness and complex refractive index for the titanium substrate and the oxide film.

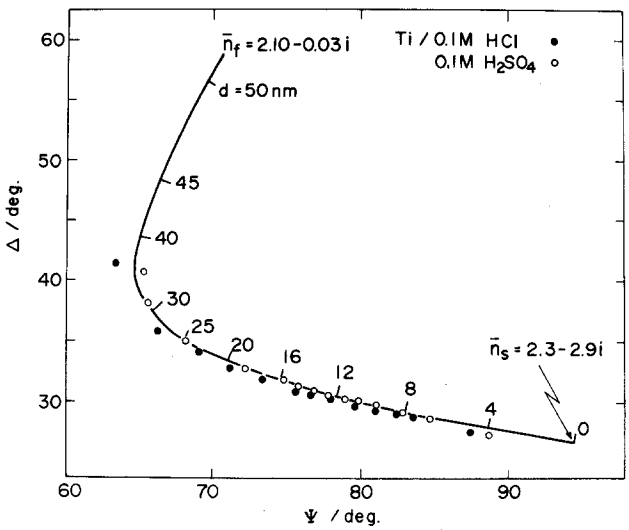

Fig. 3. Comparison between experimental Ψ and Δ measured *in situ* in 0.1*M* hydrochloric and 0.1*M* sulfuric acid solutions at an angle of incidence $\phi_1 = 70.32°$ and a theoretical Ψ *vs.* Δ curve calculated for a growing film with $\bar{n}_2 = 2.1\text{-}0.03i$ on a substrate with $\bar{n} = 2.3\text{-}2.9i$.

Film thickness.—From the results shown in Fig. 3 and 4, the film thickness can be estimated. Figure 5 and 6 show the film thickness as a function of potential in 0.1*M* HCl, and 0.1*M* H_2SO_4, and phosphate solutions. Figure 6 also shows the anodic c.d. measured after 1h polarization at constant potential. The film thickness is observed to increase almost linearly with increasing potential up to 7.5V. At potentials higher than 7.5V, the thickness increases more steeply with potential and the reproducible results of thickness measurements are hardly obtained.

In the nearly linear thickness-potential curves a slight break is observed at about 3V, showing the film thickness/potential ratio 2.6 nm V^{-1} at 0.0-3.0V, and 2.4 nm V^{-1} at 3.0-7.5V in 0.1*M* HCl solution, and 2.5 nm V^{-1} at 0.0-3.0V and 2.3 nm V^{-1} at 3.0-7.5V in 0.1*M* H_2SO_4. No such break is seen in phosphate solutions, showing the thickness/potential ratio 2.8 nm V^{-1} at 0.0-7.5V.

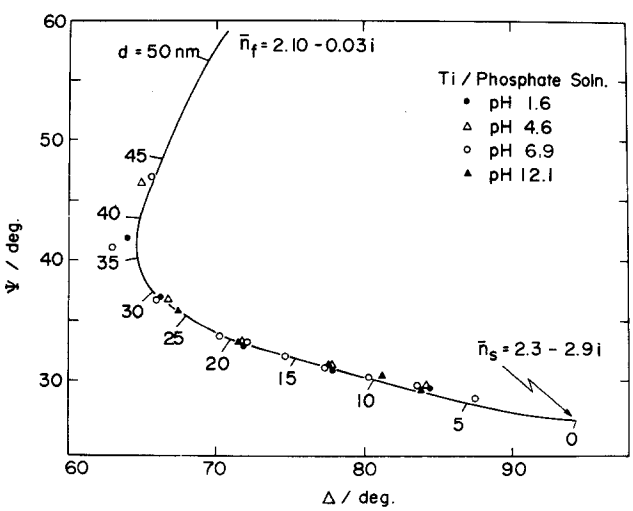

Fig. 4. Comparison between experimental Ψ and Δ measured *in situ* in phosphate solutions and a theoretical Ψ *vs.* Δ curve.

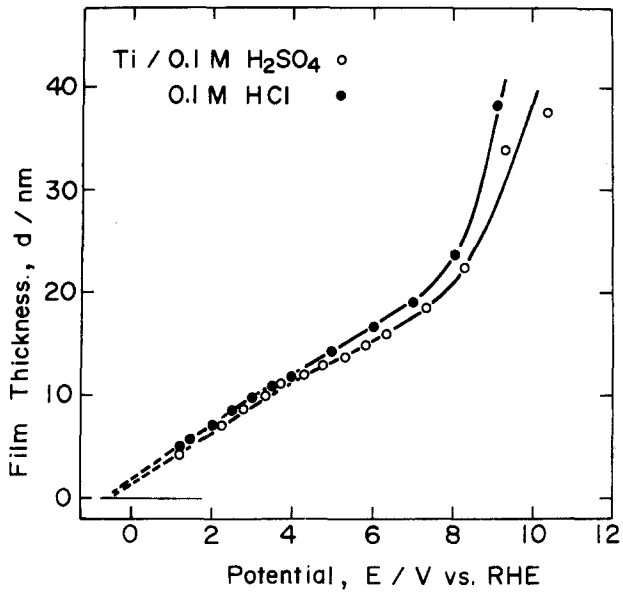

Fig. 5. Film thickness as a function of potential for the anodic oxide film formed on titanium by 1h potentiostatic oxidation in 0.1M hydrochloric and 0.1M sulfuric acid solutions.

The ratio of thickness to anodic charge passed was also measured by stepwise potential increase with a time interval of 1h. The result is shown in Fig. 7, from which the ratio is found to be 0.85 nm cm^2 mC^{-1} in pH 6.9 phosphate solutions. A slight scatter observed at 4.60V is due to the oxygen evolution reaction which consumes a part of anodic charge.

The galvanostatic film growth was also studied in pH 6.9 phosphate solution. Figure 8 shows the potential rise and film growth at constant anodic current. The thickness/charge ratio is (d/Q) = 0.68 nm cm^2 mC^{-1} at 20 μA cm^{-2} and (d/Q) = 0.71 nm cm^2 mC^{-1} at 5 μA cm^{-2}, which are smaller than the (d/Q) = 0.85 nm cm^2 mC^{-1} obtained for the potentiostatic film. This difference is probably caused by the film dissolution whose rate is dependent on the anodic c.d. (15). The linear potential rise and film growth are seen to level off at potentials more positive that 3V, where the oxygen evolution is taking place. The

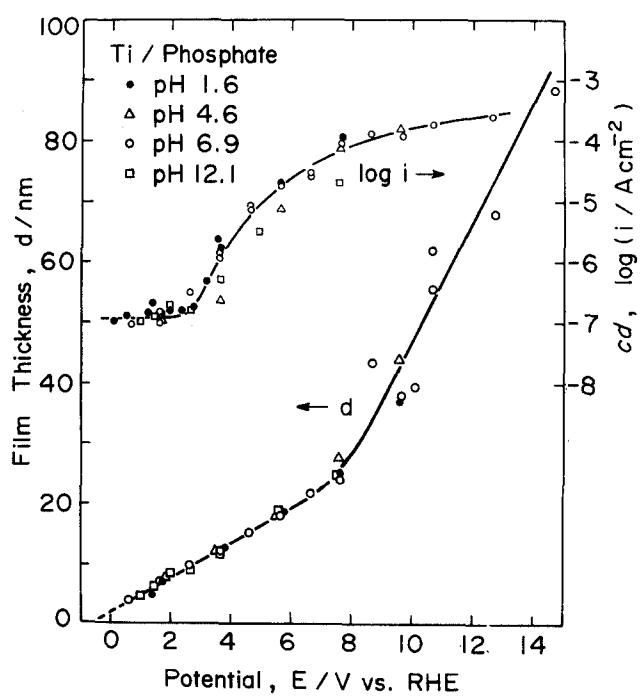

Fig. 6. Film thickness as a function of potential for the anodic oxide film formed on titanium by 1h potentiostatic oxidation in phosphate solutions at pH 1.6, 4.6, 6.9, and 12.1

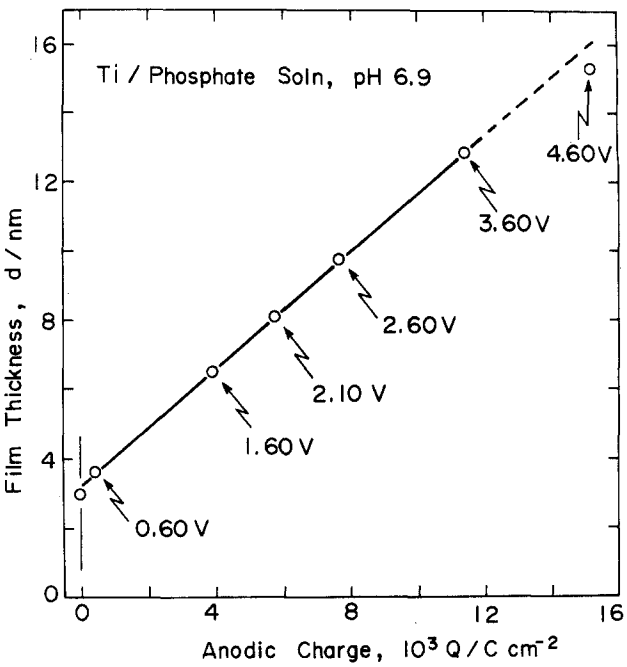

Fig. 7. Relationship between film thickness and anodic charge for the anodic oxide film on titanium by potentiostatic oxidation in pH 6.9 phosphate solution. The potential was increased stepwise at a time interval of 1h.

complex refractive index estimated for the galvanostatic film was found to be $\bar{n}_2$ = 2.10-0.03i, which is consistent with the index obtained for the potentiostatic film.

Discussion

Complex refractive index.—The conventional ellipsometry at a fixed angle of incidence requires the oxide-free metal surface to estimate the complex refractive index of the metal. Smith *et al.* attempted to estimate by conventional ellipsometry the optical constant of a titanium electrode in HF solution where any surface oxide

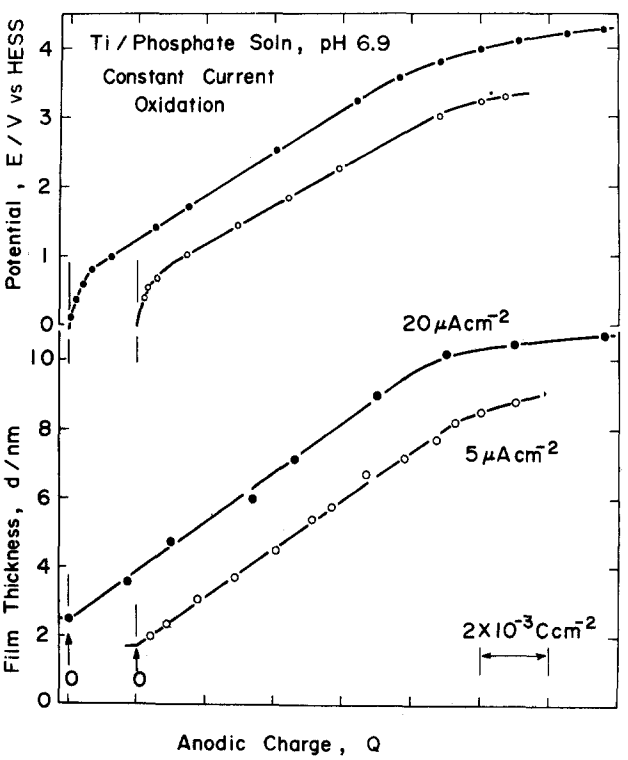

Fig. 8. Electrode potential and film thickness as functions of anodic charge passed during constant current oxidation of titanium in pH 6.9 phosphate solution.

layer would dissolve, leading to surface roughening. The electrochemical reduction of surface oxides, usually employed for iron and other metals, is incapable of producing the oxide-free bare titanium surface because of formation of surface hydride layer during cathodic reduction.

In this work, MAI ellipsometry has been employed to estimate the complex refractive index of titanium substrate covered with a surface oxide layer. This method is, in contrast with the conventional ellipsometry, capable of determining the five unknowns, n_2, k_2, d, n_3, and k_3, of a film-covered metal from a number of measurable parameters, Ψ and Δ, at different angles of incidence.

The complex refractive index of titanium at wavelength 546.1 nm found in the literature, shows some scatter (n_3 = 2.0-3.1, k_3 = 2.0-3.7), as listed in Table I. The index obtained in this work is relatively small compared with the reported values except by Andreeva (16) and Dyer *et al.* (12). It is known that the index measured by ellipsometry is sensitive to the specimen surface. In this work, the titanium specimen was slightly etched to remove a superficial polishing layer without roughening the surface.

The refractive index, n_2, of the oxide film listed in Table I shows almost no scatter except for a value reported by Laser *et al.* (8). The anodic oxide film is found to possess the refractive index smaller than that of crystalline TiO_2 whose refractive index is larger than 2.5 for anatase, rutile, and brookite (21). The small refractive index may be attributed to the hydrated structure of the anodic oxide film.

The extinction index, k_2, of the anodic oxide film obtained in this work indicates that the film is slightly light absorptive at wavelength 546.1 nm, though the film has been claimed to be transparent in literature. The slightly light absorptive nature may be explained by assuming the presence of ionic and electronic defects in the film.

Film growth.—The film growth of anodic oxide on titanium has been reported to obey the high field ion migration mechanism (22-24)

$$i = i_0 \exp(B\bar{E}) \quad [2]$$

where i_0 is ionic self-diffusion c.d. at zero field, $\bar{E}$ electric field strength, and B a constant given as follows

$$B = zaF/RT \quad [3]$$

In Eq. [3], z and a indicate, respectively, the ionic valency and the half-jump distance (or the activation distance) of migrating ion. The validity of Eq. [2] can be examined on the results of galvanostatic oxidation (Fig. 8), where the electric field is calculated from the values of $(\partial E/\partial t)$ and $(\partial d/\partial t)$.

Table I. Complex refractive indexes of titanium and its anodic oxide film

Ref.	$n = n - ki$	Remarks
	Titanium substrate (λ = 546.1 nm)	
(16)	2.10-2.02*i*	Ellipsometry
(9)	3.05-3.66*i*	Ellipsometry
(17)	2.5-3.4*i*[a]	Reflectance and transmittance spectroscopy
(18)	1.8-2.7*i*[a]	Reflectance spectroscopy
(19)	2.4-3.4*i*[a]	Reflectance spectroscopy
(12)	2.0-2.7*i*	Ellipsometry
(8)	(2.7 2.8)-(3.20 3.25)*i*	Ellipsometry
(20)	2.63-3.26*i*	Ellipsometry
Present work	2.3-2.9*i*	Ellipsometry
	Anodic oxide film (λ = 632.8 nm)	
(9)	2.5-0.0*i*	Ellipsometry
(10)	2.5-0.0*i*	Reflectometry
	Anodic oxide film (λ = 546.1 nm)	
(12)	2.1-0.0*i*	Ellipsometry
(8)	2.4-0.0*i*	Ellipsometry
(19)	2.2 (+0.05)-0.0(+0.01)*i*	Ellipsometry
Present work	2.10-0.03*i*	Ellipsometry

[a] Interpolated value.

$$\bar{E} = \left(\frac{\partial E}{\partial d}\right) = \left(\frac{\partial E}{\partial t}\right)\left(\frac{\partial d}{\partial t}\right)^{-1} \quad [4]$$

The $\bar{E}$ *vs.* i relationship is given in Fig. 9, where the closed symbol indicates the result of potentiostatic 1h oxidation. From the plot in Fig. 9, the parameters of i_0 and B in Eq. [2] are found; i_0 = 7.7 (±2.0) × 10^{-11} A cm^{-2} and B = 24 (±5) nm V^{-1}. The value of i_0 is 100 times as large as that estimated by Johansen *et al.* (22) in aqueous ammonium borate solution and by Nishimura *et al.* (23) in aqueous chloride solution. Mizushima (24) reported a larger value of i_0 in anhydrous ethylene glycol. The value of B is fairly close to that obtained by other workers (22-24). From the value of B, the half-jump distance is found to be 0.16 nm for the migration of Ti(IV) ion, which is close to one-half of the distance between neighboring Ti ions in the lattice.

Film breakdown.—The linear relationship between film thickness and potential obtained under potentiostatic conditions has been shown to break at potentials more positive than 7.5V (Fig. 5 and 6). The abrupt thickening of the film above 7.5V may be attributed to the creation of lattice defects which increase the ionic leakage current. Observation with a scanning electron microscope (SEM; JEOL JSM-255) shows nearly the same surface morphology before and after oxidation at potentials more negative than 5V. At potentials more positive than 5.5V, a crater-conglomerate morphology with a single-crater diameter of about 3 μm is observed. Such a crater-like morphology was also reported by Yahalom *et al.* (11). At potentials more positive than 7.5V, the surface becomes rough, with a ripple-like appearance. From the surface observation described above, it appears that the breakdown of the anodic oxide film commences at 5.5V, producing a number of crater-like cracks, which will provide leakage paths for ionic current. The internal compressive stress induced by high field electrostriction will play an important role in the film breakdown, as proposed in a paper by Sato (25). At potentials more positive than 7.5V, the ionic current concentrates at the cracks, forming a thick oxide layer, whose thickness for unit voltage becomes greater than that of the film formed at more negative potentials.

Film composition.—Different models for the passive film on titanium have been proposed in literature, which assume either a unilayered or a multilayered structure. In this work, the unilayered model has been adopted, since the film was found to grow up along the theoretical curve

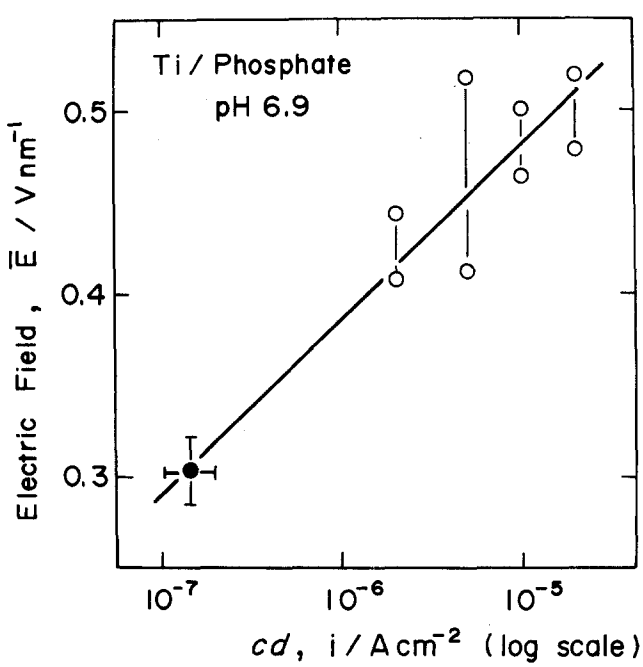

Fig. 9. Relationship between anodic current density and electric field strength for an anodic oxide film growing on titanium in pH 6.9 phosphate solution.

of the ellipsometric parameters drawn from a single-layer model.

The potential at zero film thickness is found to be $E = -0.55 \pm 0.10$V from the linear thickness-potential plot shown in Fig. 5 and 6. This potential is very close to the transition potential from Ti_2O_3 to TiO_2 (26), suggesting that the passivation film is composed primarily of TiO_2 structure. From the large value of thickness-to-charge ratio and the small refractive index, it is suggested that the anodic oxide film contains some amount of water. Yahalom *et al.* (11) and Blondeau *et al.* (27) have observed electron diffraction patterns corresponding to anatase TiO_2 for the anodic films formed at potentials more positive than 50V, where the film breakdown takes place. Blondeau *et al.* (27) have also observed a quasiamorphous structure for the anodic oxide film formed at more negative potentials.

The thickness-to-charge ratio, $d/Q = 0.85$ nm cm^2 mC^{-1}, in a potential region less positive than 3.6V is 1.5 times as large as the theoretical value, $d/Q = 0.54$ nm cm^2 mC^{-1}, calculated from the density of crystalline anatase (21), $\rho = 3.84$ g cm^{-3}, assuming the roughness factor, r, to be unity. This indicates that the anodic oxide film is hydrated. If we write the composition of the film as $TiO_2(H_2O)_y$, the content of water, y, may be calculated by Eq. [5]

$$y = \left[\left(\frac{d}{Q}\right)\left(\frac{4F\rho}{r}\right) - M_{TiO_2} \right] \frac{1}{M_{H_2O}} \qquad [5]$$

where M_{TiO_2} and M_{H_2O} are the molecular weights of TiO_2 and H_2O, respectively. By use of $(d/Q) = 0.85$ nm cm^2 mC^{-1} obtained above and $\rho = 3.2$ g cm^3 measured by Dyer *et al.* (12), we obtain $y = 1.4$ and hence the composition of the anodic oxide film to be represented by TiO_2 $(H_2O)_{1.4}$ or $TiO_{0.6}(OH)_{2.8}$. From the composition estimated above, it is evident that the film contains a large number of hydroxyl bridges in its bond structure. The presence of hydroxyl bridge may be confirmed by reversible absorption and desorption of hydrogen ions in the film observed by Dyer *et al.* (28).

Conclusion

The following conclusions may be drawn.

1. The complex refractive index at wavelength 546.1 nm is found to be $\bar{n} = 2.3\text{-}2.9i$ for the titanium substrate and $\bar{n} = 2.1\text{-}0.03i$ for the anodic oxide film formed on titanium in aqueous solution.

2. The anodic oxide film thickens linearly with increasing potential in a potential region from -0.55 to $+7.5$ *vs.* RHE under the condition of potentiostatic oxidation for 1h. The rate of thickness increase with potential is 2.8 nm V^{-1} in phosphate solutions (pH 1.6-11.5), 2.5 nm V^{-1} in 0.1*M* HCl solution, and 2.4 nm V^{-1} in 0.1*M* H_2SO_4 solution.

3. Breakdown of the anodic oxide film occurs at potentials more positive than 7.5V, beyond which a thick film is formed. The thickening of the broken film is attributed to an increased ionic leakage current at breakdown sites.

4. The anodic oxide film is represented by $TiO_2(H_2O)_{1.4}$ or $TiO_{0.6}(OH)_{2.8}$, which contains a large density of hydroxyl bridge in its bonding structure.

Manuscript submitted July 23, 1984: revised manuscript received Nov. 27, 1984.

Hokkaido University assisted in meeting the publication costs of this article.

REFERENCES

1. R. D. Armstrong and R. E. Firman, *J. Electroanal. Chem.*, **34,** 391 (1972).
2. E. J. Kelly, in "Proceedings 5th International Congress on Metallic Corrosion," N. Sato, Editor, p. 137, NACE, Houston, TX (1974); *This Journal,* **123,** 162 (1976).
3. E. J. Kelly, *ibid.*, **126,** 2064 (1979).
4. J. P. Frayret, R. Pointean, and A. Caprani, *Electrochim. Acta,* **26,** 1783 (1981); *ibid.*, **26,** 1789 (1981).
5. C. Caprani and J. P. Frayret, *ibid.*, **24,** 835 (1979).
6. J. J. Kelly, *ibid.*, **24,** 1273 (1979).
7. J. A. Harrison and D. E. Williams, *ibid.*, **27,** 891 (1982).
8. D. Laser, M. Yaniv, and S. Gottesfeld, *This Journal,* **125,** 358 (1978).
9. T. Smith and F. Mansfeld, *This Journal,* **119,** 663 (1972).
10. J. F. McAleeer and L. M. Peter, *ibid.*, **129,** 1252 (1982).
11. J. Yahalom and J. Zahavi, *Electrochim. Acta,* **15,** 1429 (1970).
12. C. K. Dyer and J. S. L. Leach, *This Journal,* **125,** 1032 (1978).
13. T. Ohtsuka, *Bull. Jpn. Inst. Metals,* **20,** 614 (1981).
14. K. Kudo and N. Sato, *Bull. Fac. Eng. Hokkaido Univ.,* **61,** 45 (1971).
15. K. D. Allard and K. E. Heusler, *J. Electroanal. Chem.,* **77,** 35 (1977).
16. V. V. Andreev, *Corrosion NACE,* **20,** 37 (1964).
17. P. B. Johnson and R. W. Christy, *Phys. Rev. B.,* **9,** 5056 (1974).
18. D. W. Lynch, C. G. Olson, and S. H. Weaver, *ibid,* **11,** 3617 (1975).
19. G. Blondeau, M. Froelicher, M. Froment, and A. Hugot-Le Goff, *Thin Solid Films,* **38,** 261 (1976).
20. C. P. De Pauli, M. C. Giordano, and J. O. Zerbino, *Electrochim. Acta,* **28,** 1781 (1983).
21. "CRC Handbook of Chemistry and Physics," 61st., ed., R. C. Weast, Editor, p. B-159, CRC Press Inc., Boca Raton, FL (1980).
22. H. A. Johansen, G. B. Adams, Jr., and P. Van Ryssel-berghe, *This Journal,* **104,** 339 (1957).
23. R. Nishimura and K. Kudo, *Corros. Sci.,* **22,** 637 (1982).
24. W. Mizushima, *This Journal,* **108,** 825 (1961).
25. N. Sato, *Electrochim. Acta,* **16,** 1683 (1971).
26. P. Pourbaix "Atlas of Electrochemical Equilibria in Aqueous Solution," Pegamon Press, Oxford (1966).
27. G. Blondeau, M. Froelicher, M. Froment, A. Hugot- Le Goff, M. Brien, R. Calsou, and P. Larroque, *J. Microsc. Spectrosc. Electron.* **2,** 27 (1977).
28. C. K. Dyer and S. S. L. Leach, *Electrochim. Acta,* **23,** 1387 (1978); *This Journal,* **125,** 23 (1978).